2024 IEEE/RSJ International Conference on Intelligent Robots and Systems (IROS)
October 14-18, 2024. Abu Dhabi, UAE

Embedded Valves for Distributed Control of Soft Pneumatic Actuators

1st Runze Zuo
Mechanical Engineering
University of Michigan
Ann Arbor, United States
zuorunze@umich.edu

2nd Mayank Mehta
Mechanical Engineering
University of Michigan
Ann Arbor, United States
mayanknm@umich.edu

3rd Dong Heon Han
Mechanical Engineering
University of Michigan
Ann Arbor, United States
dongheon@umich.edu

4th Daniel Bruder
Mechanical Engineering
University of Michigan
Ann Arbor, United States
bruderd@umich.edu

***Abstract*—Soft robotic systems are inherently compliant, giving them unique capabilities not possessed by traditional rigid-bodied robot systems. Many soft systems rely on soft pneumatic actuators. One of the biggest downsides of such actuators is the need for bulky pressure-regulating devices and individual pneumatic supply lines. In this work, a miniaturized pressure-regulating system is developed and embedded into the unused space inside of a soft pneumatic McKibben actuator, enabling the simultaneous pressure control of multiple actuators connected to a single pneumatic supply line. This "valve-embedded" actuator is capable of regulating its internal pressure within 0.05 psi of a desired set point, even under external load. Compared to a conventional McKibben actuator driven by external valves, the valve-embedded actuator is experimentally shown to consistently achieve faster settling times. To showcase the practical application of the valve-embedded actuator on a robotic system, a 0.9m serial-linked robot driven by five independently controlled valve-embedded actuators was assembled, and was shown to achieve an average root mean square error of less than 1.5cm in a waypoint tracking experiment. The miniaturized pressure control system developed in this work is open source and could be embedded in any fluid-driven actuator, enabling more capable and densely actuated pneumatic soft robots.**

***Index Terms*—Soft material robotics, McKibben pneumatic actuators, valve and control embedded actuator, pressure control**

I. Introduction

Soft Pneumatic Actuators (SPAs) have been a popular actuation technology in the soft robotics community for decades. They can deliver significant force relative to their weight, which is beneficial for lightweight applications such as wearable robotics [1], [2]. Their inherent compliance further allows them to adapt to varied and unstructured environments, enabling applications such as handling fragile objects [3], [4] or navigating rugged terrain [5], [6], where rigid robots face limitations. Moreover, their compliance makes them safer in collaborative tasks where robots work alongside humans [7], [8]. These benefits, combined with the low cost of fabrication, quick response times, and easy implementation, demonstrate the potential SPAs can offer towards building safe and responsive robots [9], [10].

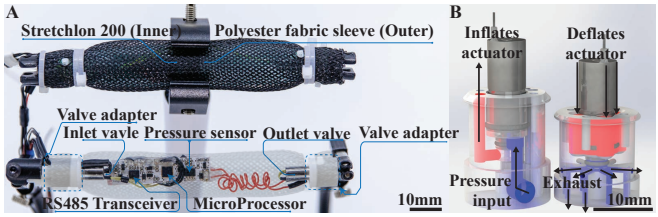

Fig. 1. (A) Photo of the proposed valve-embedded actuator. The upper part shows the external look of the actuator, while the lower part demonstrates the internal components including valve adapters, miniature solenoid valves, and the flexible PCB that houses the sensing, control, and communication electronics. (B) Rendered picture of the valve adapters (left: inlet; right: outlet).

However, a significant challenge to their widespread application is the complexity of managing a large number of parallel pneumatic channels as the number of SPAs scales up. The weight addition from long pneumatic channels and valves further restricts the portability of SPA-based soft robots, requiring most of them to be tethered to external valves and power supplies.

Researchers have explored multiple modalities to tackle this "piping challenge" of connecting each actuating unit with the pressure source and modulating the pressure in each unit. Microfluidics-based demultiplexers [11], [12] and random-access memory [13] have been used to make lighter fluidic control interfaces by using a lower number of control lines to actuate a higher number of actuators. Shape Memory Alloy (SMA) based pinch valves have also been explored to develop a miniaturized fluidic control board to effectively control the pneumatic flow in multiple lines by selectively controlling a micro-valve by on-board Joule heating via passing current [14], [15] or wirelessly heating via electromagnetic induction [16]. However, both approaches require specialized fabrication methods and lack the reprogrammability of electronic microcontrollers. Moreover, the microfluidic systems must also refresh the state of each valve periodically to nullify the effects of pneumatic memory degradation. The SMA-based systems are also limited in their switching frequencies due to the time it takes them to cool. To reduce the total

weight of electronic and pneumatic components in multiple parallel pneumatic channels, researchers have also leveraged acoustic resonance to selectively actuate pneumatic valves by combining the traditionally separate pneumatic power line and electronic signal line into a single pneumatic line doubling as both a power and control channel [17]–[19]. However, these systems are highly susceptible to noise and attenuation at longer distances and in pneumatic channels that are not straight.

A promising approach to tackle the piping problem in soft robots that require a high density of SPAs is the modularization of SPAs by integrating valves and sensing with the actuator to reduce the number of pneumatic and control lines. This approach has been previously used to miniaturize a hydraulically actuated McKibben muscle for minimally invasive surgery [20]. However, the implementation lacks universality and reproducibility, as it relied on a custom miniature valve explicitly designed for the intended application. One of the earliest works with integrating pressure control and sensing into a single McKibben muscle was proposed by Jien *et al.* [21]. However, the form factor of the integrated actuator is not compact enough to mitigate the scaling challenge. More recently, Booth *et al.* [22] proposed an integrated pressure regulator designed for pneumatically driven soft robots to overcome pressure differences caused by manufacturing variability in soft actuators by decentralizing pressure control to tackle local disturbances effectively. However, the proposed fluid control board has a bulky form factor that interferes with the soft dynamics of the robot.

In this paper, we overcome the piping problem by embedding valves, pressure sensors, and control units directly inside pneumatic actuators. We propose a standalone, modular McKibben actuator (Fig. 1) integrated with valves, sensing, and control units. This modular McKibben actuator alleviates the piping problem in soft robotic systems requiring high-density SPA units, as each unit can be connected via small pneumatic channels to a single pneumatic supply tube. Moreover, pressure regulation in long pneumatic transmission lines requires complex modeling and characterization of pipe dynamics to implement pressure estimation and control at a distal pneumatic actuator [23]–[25]. The proposed modularized system directly measures and controls the pressure at each unit, leading to a simpler, faster, and more accurate pressure control. Furthermore, the proposed valve design utilizes the unused space inside the McKibben actuator, giving rise to a sleek and convenient form factor without (or minimally) affecting the actuator's soft dynamics. The embedded design is entirely composed of off-the-shelf components and 3D printed parts and all code is open-source. This makes the proposed approach readily reproducible, opening the door for the widespread development of more capable pneumatic soft robots.

II. Valve-Embedded Actuator Design

A. Overview of the Design Concept

The primary design goal is to improve the placement flexibility and density of actuators within a robotic system. This objective is achieved by integrating the regulator directly into the actuator, thereby eliminating the need for tubing connecting each actuator to an external regulator. As depicted in the schematic of the system in Figure 2B, Each actuator receives constant pressure from a shared pneumatic bus, subscribes to command by connecting to a shared communication bus, and powers itself from the shared voltage rails. This configuration simplifies the robotic system architecture to require only four wires and one tube running along the robot, enabling actuators to be easily installed and utilized anywhere on the robot. We also carefully designed the components of the regulator to ensure that the form factor of the enhanced actuator remains comparable to that of traditional actuators without an integrated regulator. Detailed mechanical and electrical designs are discussed in the subsequent sections.

B. Mechanical Design

Figure 1 presents the internal configuration of the actuator. On the bottom end, a Stereolithography (SLA) 3D printed part is used as the inlet adapter, McKibben sealing cap, wire guide, and valve housing at the same time. This multifunctional design reduces the actuator's dead volume. A common challenge with SLA-printed components is their insufficiently smooth surface for effective O-ring sealing. To address this, we printed the part with a machinable material (Accura Xtreme White 200) and used the precision spiral reamer on the lathe to reach a smooth side-wall finish. For the actuator's inlet and outlet valves, we selected the 7mm SV series miniature solenoid valve from Clippard. While the Parker X-Valve is another widely used option in soft robotics research, the SV series offers a superior flow rate at 40 psi. Moreover, the O-rings integrated ports facilitate a more compact system design. The actuator's mesh and inner tubing configuration is adopted from previous work [26]. The fiber mesh is cut from commercially available braided Polyester Fabric sleeving. The inner tubing is fabricated using Stretchlon 200 bagging film, a commercial thermoplastic polyurethane (TPU) film that is lightweight and heat-sealable.

The regulator-embedded McKibben actuator exhibits a contraction ratio of 30% when pressurized to 40 psi with a 1 kg load (see Fig. 5A) This is comparable to the contraction ratio of conventional non-embedded McKibben actuators [27], [28], indicating that the embedded valves do not significantly restrict the deformation of the actuator.

C. Electrical Design and Closed-Loop Pressure Controller

The control module embedded within the actuator is designed to fulfill the following functions: driving the solenoid valves, sensing the actuator's internal pressure, and receiving commands from the communication bus. We choose to use

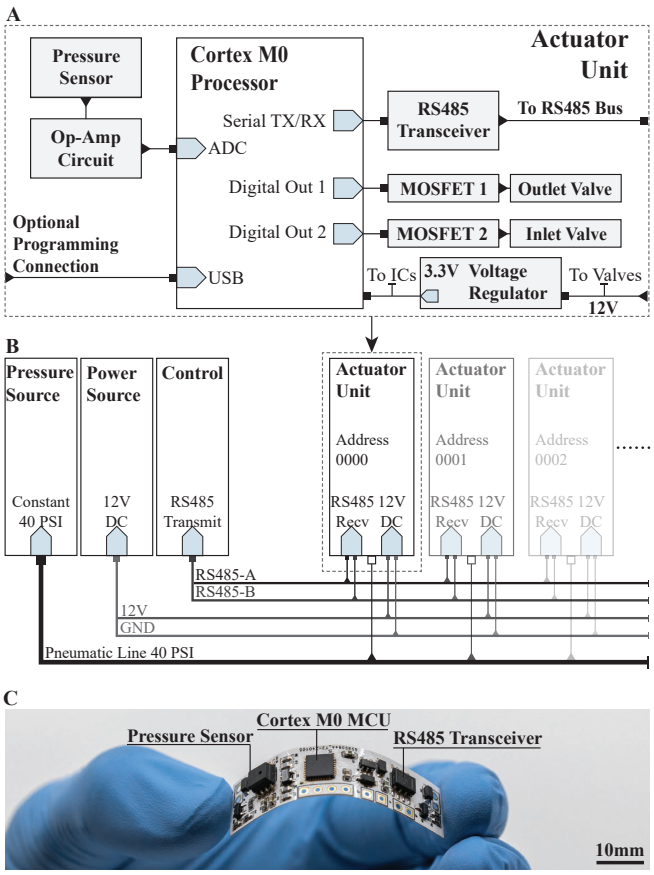

Fig. 2. (A) Schematic for the control circuit inside an actuator unit. (B) An example layout for using the proposed actuator on a robot system. Each actuator unit can be placed on a bus, sharing common pressure/power/control sources. (C) A photo of the control circuit inside the actuator. The PCB is made with flexible material to maintain the structural compliance of the McKibben actuator.

the ATSAMD21E18 Cortex M0+ microprocessor due to its compact size, energy efficiency, and sufficient computational capability. Each valve is driven by an NMOS switching circuit. A pair of these circuits is positioned at either end of the flexible circuit board. The pressure inside the actuator is detected by an NPP-301A-700A pressure sensor, which produces a differential voltage output in the range of 0-60mV. The differential voltage is then amplified by an operational amplifier circuit, which scales the signal to a 0-3.3V range suitable for sensing by the analog-digital converter (ADC) on the microprocessor. We choose to use RS485 as the bus communication protocol. It has desirable features such as long operating distance, high data rates, and dependable signal integrity in noisy environments. An RS485 transceiver is thus incorporated onto the board, and connected to the serial communication port of the microprocessor.

The pressure is regulated by a bang-bang controller. It turns on the inlet valve if the pressure is below the set point, turns on the outlet valve if above the set point, and deactivates both valves if at ± 0.05 psi from the set point. For each program loop, the microprocessor polls commands from the RS485 bus. This time-consuming activity affects the timeliness of pressure monitoring and valve control. To mitigate this, we leverage the microprocessor's timer interrupt to maintain the frequency of the pressure-regulating control loop. The timer interrupt handler is programmed to sense the pressure and modulate the valves. This handler is executed twice for each timer period: upon timer overflow and at a predetermined timer count, both of which are configurable. Such configurability enables the potential application of Pulse Width Modulation (PWM) for the valves, mimicking the behavior of proportional valves by modulating the valve 'on' time. In this work, we will only use a bang-bang controller, as its pressure control performance on an on/off valve is comparable to the PWM method [29]. In the future, PWM can be added to achieve smoother robot kinematics.

III. Experiments

A. Valve-Embedded McKibbens vs Conventional McKibbens

Conventional McKibben actuators rely on external pressure regulators to operate. In most cases, it is not feasible to incorporate the bulky regulators directly into the robot. Long pneumatic lines are required to connect the McKibben actuators to the external regulator. As the robot scales up or the density of actuator placement on a robot increases, it is required to use longer tubing; or tubing with smaller inner diameters if the robot needs to be compact. We are interested in quantitatively determining how the length of the tubing will affect the performance of the conventional actuator in terms of control delay and pressure tracking error, and how well our proposed valve-embedded actuators solve this issue.

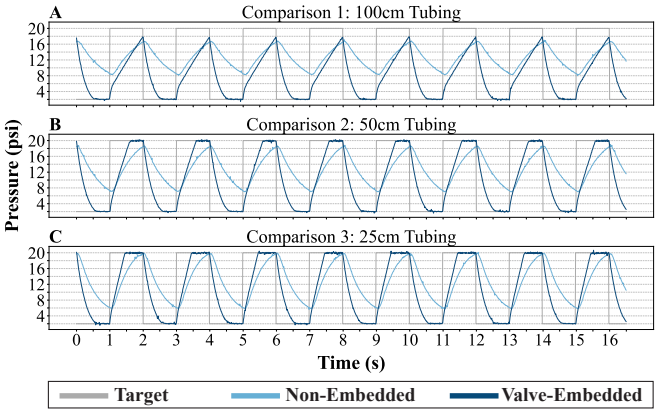

Fig. 3. Comparison experiment between the valve-embedded McKibben actuators and the conventional non-embedded McKibben actuators. Both actuators are programmed to track a square wave 2-20 psi, 0.5Hz input signal. The tubing used has an inner diameter of 1/32 inch. In terms of tracking error, our actuator is 37% better when using a 100 cm 1/32 inch inner diameter tubing, 51% better for 50cm tubing, and 53% better for 25cm tubing (A) Tracking result comparison when the actuator is connected to the pressure source with 100cm tubing. (B) Same experiment using 50cm tubing. (C) Same experiment using 25cm tubing.

In our comparison experiment, we constructed two McKibben actuators. The first one is the proposed valve-embedded actuator with two valves and a control board (with pressure sensor) inside. The second one does not have the valves embedded, however, it has a pressure sensor placed inside the actuator to acquire actual internal pressure. The external pressure regulator of the non-embedded actuator is the Enfield TR Electronic Pressure Regulator. It is a closed-loop pressure regulator using the pressure sensor at the output port as the feedback.

Three experiments are performed using lengths of 100cm, 50cm, and 25cm tubing to connect the actuators to their compressed air source. The tubing is a PVC soft plastic tubing with an inner diameter of 1/32 inch and an outer diameter of 3/32 inch. In all three experiments, both actuators are tasked to track a square wave input signal with 2-20 psi magnitude and 0.5 Hz frequency. The actual pressure curves for both actuators are collected using their internal pressure sensor and are plotted onto figure 3. In figure 3A, due to the fluid resistance introduced by the 100cm tubing, both actuators cannot reach the 20 psi target in under one second. However, the deflating performance of the valve-embedded actuator drastically outperforms the conventional actuator. This is because the valve-embedded actuator vents pressure directly to the atmosphere without needing to go through the 100cm tubing. In figure 3B and C, the valve-embedded actuator can consistently reach and maintain the set points of 2 psi and 20 psi, whereas the conventional actuator struggled to achieve 20 psi with 25cm tubing and failed to reach 2 psi in all tests. The valve-embedded actuator exhibited no noticeable control delay, whereas the conventional actuator showed a 100-millisecond delay for both inflate and deflate in the 100cm tubing experiment.

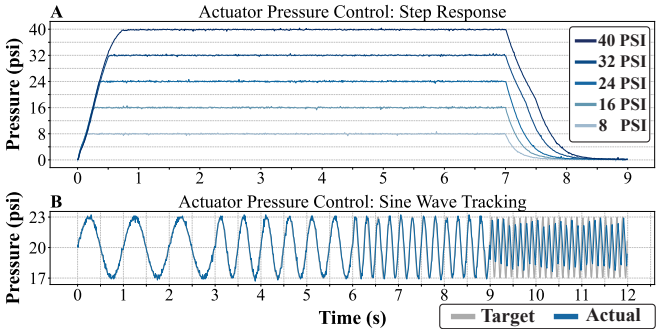

Fig. 4. (A) The Actuator is programmed to follow a step target signal from 8 psi to 40 psi. (B) The actuator tracks a sine wave target signal, with the frequency starting at 1 Hz, and then increased to 2 Hz, 4 Hz, and 8 Hz

B. Characterization of the Valve-Embedded Actuators

To characterize the performance of the valve-embedded McKibben actuator, we assembled a 10cm variation of the actuator (10cm is the fully stretched length of the inflatable part of the actuator at 0 psi, excluding the bottom and cap adapters.) and connected it to a 42 psi constant pressure source. We set the target signal to be steps with heights of 8, 16, 24, 32, and 40 psi and let the actuator track the step signal. In figure 4A, we plotted the step-tracking response of the actuator. The pressure rising speed is measured to be 64 psi per second from 0 to 32 psi range. Beyond 32 psi, the rate slows due to the proximity to the 42 psi supply pressure. There is no observable overshoot because the bang-bang controller is running at 400 Hz and the switching speed of the valve is very fast (<5ms) The steady-state tracking drift is 0.045 psi with an average oscillating error of 0.104 across the operating pressure range (0-40 psi). The source of the tracking error is likely the precision loss during the microcontroller's floating point calculations and ADC conversions. Figure 4B shows the actuator's ability to follow a sinusoidal pressure target. The target sinusoid starts with a magnitude of 3 psi, an offset of 20 psi, and a frequency of 1 Hz. For every 3 seconds, the target sinusoid escalates its frequency. From the figure, we observe that the proposed actuator can track the signal quite closely up to 4 Hz at the shown 20 psi offset and 3 psi magnitude.

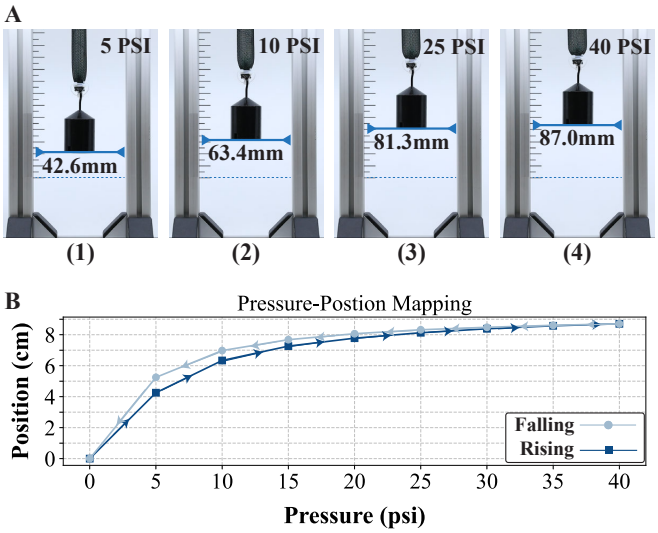

Fig. 5. A longer (30cm) variation of the actuator is lifting a 1 kg payload. (A) Photos of the actuator's contraction position at different pressures. (B) The position curve of the payload when the internal pressure of the actuator starts at 0 psi, rises with a step of 5 psi, stops at 40 psi, and then falls to 0 psi with each step at 5 psi.

To verify that the embedded control system works under load, we measured the displacement versus pressure of a valve-embedded McKibben actuator with a weight hanging from it. A longer 30cm length actuator was built for this experiment to enable more visible contractions. One end of the actuator is fixed to a frame, with the other end attached to a 1 kg payload. The pressure control sequence starts at 0 psi and rises in 5 psi increments. For each step, we wait until the position stabilizes and then measure the lifted distance of the payload. Figure 5A demonstrates steady-state position at

5, 10, 25 and 40 psi when the actuator is lifting the payload. After reaching 40 Psi, the pressure falls back to zero with a decrement of 5 psi per step. The position is plotted against the pressure to generate figure 5B. We can observe hysteresis in this rising-falling cycle. This is a common trait for the McKibben actuators because of the inter-component friction [30].

C. Demonstration of the Actuators on a Serial-Linked Arm

To illustrate the practical application of the valve-embedded actuator in robotic systems, we built a serial-linked planar robotic arm with five links as shown in figure 6.

Each segment of the arm has one valve-embedded actuator and a spring. One end of the actuator is connected to the base of the link, while the other end is connected to the base of the next link. The spring is installed on the opposite direction with the actuator to resist deviations from the arm's resting configuration. Two adjacent segments are linked together using a hinge structure. With this configuration, each actuator can independently control the joint angle between its link and the next link. Because of the hysteresis observed in the previous experiment, measuring internal pressure is not sufficient to accurately infer the joint angles. Therefore, we placed an ArUco marker [31] on each link and used a camera to capture the orientation of the marker to get the angle of each joint. For each joint, a PID controller is used to track the joint angle by modulating the actuator's internal pressure. The first task shown in Fig 6B is to move the end-effector to a series of predefined waypoints. After a target waypoint is given, at each time-step, the controller calculates the analytic Jacobian matrix [32] for the current configuration. The Jacobian maps an incremental change in end-effector position pointing toward the desired waypoint to a corresponding change in joint angles. Then, the PID controller at each joint induces the incremental change in joint angles. By repeating this process, the robot will iteratively reach the target waypoint.

The second task (shown in Fig 6C) is to follow an "M" shaped trajectory using the tip of the arm. The same iterative Jacobian controller is used to complete this task. From the demo, we can see that the serial-linked arm using the proposed valve-embedded actuator can accurately control the end-effector location with a steady state root-mean-squared tracking error of 1.5cm, thereby showcasing the effectiveness of the valve-embedded actuators in robotic applications.

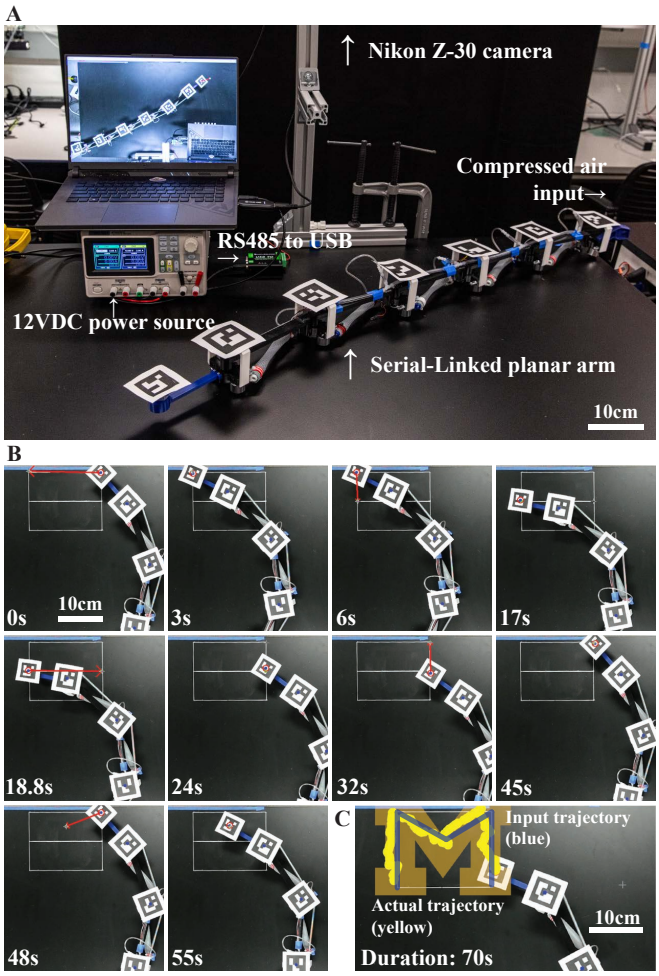

Fig. 6. Demonstration of the valve-embedded actuators on a serial-linked planar robotic arm. (A) Robot setup: The pressure input is at a constant 42 psi, regulated from the laboratory compressed air. The voltage source is set to 12V DC. The USB to RS485 converter delivers commands from the PC to the RS485 busline. (B) This figure demonstrates the arm completing a waypoint tracking task. The robot arm can place its end-effector in the desired location. Each joint is driven by one actuator and is independently closed-loop controlled using the ArUco Markers to acquire joint angle feedback, and the desired joint angles are iteratively updated using the Jacobian inverse dynamic controller. (C) The robot can follow a preset trajectory. An 'M' shaped trajectory is given in blue, and the actual robot trajectory is shown in yellow in the figure.

IV. Discussion

Through the comparison experiment between the newly designed actuator and the traditional McKibben actuator, we have shown that our actuator outperforms the traditional McKibbens by a large margin. Specifically, in terms of pressure tracking error against the target signal, our actuator is 37% better when connected to a pressure source through a 100 cm length of 1/32 inch inner diameter tubing, 51% better for a 50cm length of tubing, and 53% better for a 25cm length of tubing.

Characterization experiments have shown that the proposed valve-embedded actuator has an effective range of 0 psi to 40 psi. Across the whole range, the steady state average tracking error is 0.045 ± 0.1064 psi. Additionally, a pressure-contraction mapping experiment has demonstrated that the proposed actuator has a 30% contraction ratio at 40 psi, similar to the contraction ratio that a conventional McKibben would achieve. Finally, a serial-linked planar robot arm is assembled using the proposed actuator. We have demonstrated

that the actuators can operate simultaneously on a single bus line and precisely navigate the end-effector of the arm with an average steady-state tracking error of 1.5cm. A video of the serial-linked arm navigating through the waypoints and drawing the "M" pattern is available in the supplementary video attached to this paper.

Despite the obvious advantages, shortcomings also exist by moving the valves and the control board inside the actuator. The primary limitation arises from the use of commercial valves, which typically have limited orifice sizes that can impede the speed of pressure adjustment. Another concern is the durability of the flexible control board. The metallic conductors within the board are susceptible to work hardening and stress accumulation. The actuator's lifespan might be affected due to this reason. These shortcomings can be addressed through future engineering efforts. The recent development of fluidic amplifiers [33], [34] is one of the promising ways to increase the flow rate while keeping the compact form factor. The control board can also be made more flexible by implementing custom-cut patterns and more resistant to stress accumulation by using curved traces.

V. Conclusion

In this paper, we present a novel design of a McKibben actuator with internally embedded inlet and outlet valves, and an internally installed flexible PCB with a pressure sensor, an RS485 transceiver, a microprocessor, and two valve driver MOSFET switching circuits. Utilizing the internal components, the proposed actuator can receive target pressure from the communication bus, and use the pressure sensor and the inlet/outlet valves to regulate its internal pressure in a closed-loop manner. Therefore, the proposed actuator can operate using a constant pressure and voltage input. This enables multiple actuators to be connected to a shared bus line, eliminating the need for separate pneumatic lines for each actuator.

Performance-wise, this proposed McKibben actuator with embedded valve, sensing, and control demonstrates significant advantages over its traditional counterparts. The pneumatic line is already at constant high pressure (42 psi in this work) at the input port of the valve-embedded actuator. When regulating the internal pressure, the pressure of the valve-embedded actuator can change almost instantly because the pressure only needs to travel through the valve. In contrast, conventional McKibben actuators rely on external regulators, from which the pressure must propagate through the pneumatic line to reach the actuator. Consequently, our valve-embedded McKibbens are much more responsive than the conventional McKibbens. Furthermore, our proposed actuator is also embedded with a pressure sensor and a high-performance microcontroller. The sensor can capture the real-time, accurate internal pressure of the actuator from within, whereas the conventional actuator's pressure can only be measured from across the pneumatic line. Using the timer interrupt, the microcontroller runs the pressure control loop at 400 Hz. This high-frequency loop facilitates agile pressure tracking, significantly reducing overshoots and steady-state control errors. This is made possible by distributing the processing resource to each single actuator.

Application-wise, the conventional McKibben actuators incur a significant volume overhead due to the reliance on external regulators and separate pneumatic lines. Our enhanced McKibben actuator addresses this issue by incorporating the regulator within its structure, thus significantly reducing the volume overhead. Additionally, the bus structure allows the actuator to be added to the robotic system without the need to allocate dedicated space for the additional tubing.

Manufacture-wise, this proposed actuator only uses off-the-shelf components, and we open-sourced all the PCB and 3D design files (https://github.com/free-laboratory/valve-embedded-McKibben). This makes our proposed approach easily reproducible for interested researchers. Furthermore, although this work focuses on embedding valves, sensing, and controls into a McKibben Actuator, the same components can be embedded in any type of fluid-driven actuator by altering the shape of the 3D-printed parts.

Combining performance superiority, application flexibility, and manufacturing simplicity, our proposed actuator can be utilized to build sophisticated robotic systems. Such systems can have high actuator placement density, minimal external regulating devices, and uncompromising actuator performance. For example, it is possible to use our actuator to build untethered systems that are powered with a single pressurized reservoir and a small battery, making these systems less encumbered by the bulky infrastructure typically associated with pneumatic actuation. It is also possible to build an over-actuated soft robotic arm and leverage the control freedom gained through a large amount of individually controllable actuators. For example, such a soft arm could utilize the recently developed variable antagonistic stiffening model [26] to achieve unprecedented performance in terms of payload capacity and posture control. In this way, we believe that the capabilities enabled by valve-embedded soft actuators will lead to the development of more capable fluid-driven soft robots.

VI. Acknowledgement

The authors would like to recognize Charlie Bradley and the University of Michigan machine shop staff for their fabrication assistance. The first author would also like to thank Min Zuo, Jing Gu, and Yuqin Kewang for their additional support.

References

[1] P. Polygerinos, Z. Wang, K. C. Galloway, R. J. Wood, and C. J. Walsh, "Soft robotic glove for combined assistance and at-home rehabilitation," *Robotics and Autonomous Systems*, vol. 73, pp. 135–143, 2015.

[2] Y.-L. Park, B.-r. Chen, N. O. Pérez-Arancibia, D. Young, L. Stirling, R. J. Wood, E. C. Goldfield, and R. Nagpal, "Design and control of a bio-inspired soft wearable robotic device for ankle–foot rehabilitation," *Bioinspiration & biomimetics*, vol. 9, no. 1, p. 016007, 2014.

[3] G. Gao, C.-M. Chang, L. Gerez, and M. Liarokapis, "A pneumatically driven, disposable, soft robotic gripper equipped with multi-stage, retractable, telescopic fingers," *IEEE Transactions on Medical Robotics and Bionics*, vol. 3, no. 3, pp. 573–582, 2021.

[4] N. R. Sinatra, C. B. Teeple, D. M. Vogt, K. K. Parker, D. F. Gruber, and R. J. Wood, "Ultragentle manipulation of delicate structures using a soft robotic gripper," *Science Robotics*, vol. 4, no. 33, p. eaax5425, 2019.

[5] R. F. Shepherd, F. Ilievski, W. Choi, S. A. Morin, A. A. Stokes, A. D. Mazzeo, X. Chen, M. Wang, and G. M. Whitesides, "Multigait soft robot," *Proceedings of the national academy of sciences*, vol. 108, no. 51, pp. 20 400–20 403, 2011.

[6] S. Chen, Y. Cao, M. Sarparast, H. Yuan, L. Dong, X. Tan, and C. Cao, "Soft crawling robots: design, actuation, and locomotion," *Advanced Materials Technologies*, vol. 5, no. 2, p. 1900837, 2020.

[7] Y. Ansari, M. Manti, E. Falotico, Y. Mollard, M. Cianchetti, and C. Laschi, "Towards the development of a soft manipulator as an assistive robot for personal care of elderly people," *International Journal of Advanced Robotic Systems*, vol. 14, no. 2, p. 1729881416687132, 2017.

[8] C. Firth, K. Dunn, M. H. Haeusler, and Y. Sun, "Anthropomorphic soft robotic end-effector for use with collaborative robots in the construction industry," *Automation in Construction*, vol. 138, p. 104218, 2022.

[9] M. S. Xavier, C. D. Tawk, A. Zolfagharian, J. Pinskier, D. Howard, T. Young, J. Lai, S. M. Harrison, Y. K. Yong, M. Bodaghi *et al.*, "Soft pneumatic actuators: A review of design, fabrication, modeling, sensing, control and applications," *IEEE Access*, vol. 10, pp. 59 442–59 485, 2022.

[10] G. M. Whitesides, "Soft robotics," *Angewandte Chemie International Edition*, vol. 57, no. 16, pp. 4258–4273, 2018.

[11] N. W. Bartlett, K. P. Becker, and R. J. Wood, "A fluidic demultiplexer for controlling large arrays of soft actuators," *Soft matter*, vol. 16, no. 25, pp. 5871–5877, 2020.

[12] D. W. Lee, I. Doh, Y. Kim, and Y.-H. Cho, "Advanced combinational microfluidic multiplexer using multiple levels of control pressures," *Lab on a chip*, vol. 13, no. 18, pp. 3658–3662, 2013.

[13] S. Hoang, K. Karydis, P. Brisk, and W. H. Grover, "A pneumatic random-access memory for controlling soft robots," *Plos one*, vol. 16, no. 7, p. e0254524, 2021.

[14] C. M. Pemble and B. C. Towe, "A miniature shape memory alloy pinch valve," *Sensors and Actuators A: Physical*, vol. 77, no. 2, pp. 145–148, 1999.

[15] S. Vyawahare, S. Sitaula, S. Martin, D. Adalian, and A. Scherer, "Electronic control of elastomeric microfluidic circuits with shape memory actuators," *Lab on a Chip*, vol. 8, no. 9, pp. 1530–1535, 2008.

[16] M. M. Ali and K. Takahata, "Wireless microfluidic control with integrated shape-memory-alloy actuators operated by field frequency modulation," *Journal of Micromechanics and Microengineering*, vol. 21, no. 7, p. 075005, 2011.

[17] A. Kitagawa, S. Jing, C. Liu, and H. Tsukagoshi, "A study on a sound operated valve for a wearable pneumatic system," in *Proceedings of the JFPS International Symposium on Fluid Power*, vol. 2008, no. 7-2. The Japan Fluid Power System Society, 2008, pp. 433–438.

[18] Y. Nishioka, K. Suzumori, T. Kanda, and S. Wakimoto, "A new control method utilizing multiplex air vibration for multi-dof pneumatic mechatronics systems," in *2010 IEEE/RSJ International Conference on Intelligent Robots and Systems*. IEEE, 2010, pp. 3037–3042.

[19] K. Suzumori, N. Osaki, J. Misumi, A. Yamamoto, and T. Kanda, "A multiplex pneumatic actuator drive method based on acoustic communication in air supply line," in *2014 IEEE/RSJ International Conference on Intelligent Robots and Systems*. IEEE, 2014, pp. 2795–2800.

[20] A. Moers, M. De Volder, and D. Reynaerts, "Integrated high pressure microhydraulic actuation and control for surgical instruments," *Biomedical microdevices*, vol. 14, pp. 699–708, 2012.

[21] S. Jien, S. Hirai, Y. Ogawa, M. Ito, and K. Honda, "Pressure control valve for mckibben artificial muscle actuators with miniaturized unconstrained pneumatic on/off valves," in *2009 IEEE/ASME International Conference on Advanced Intelligent Mechatronics*. IEEE, 2009, pp. 1383–1388.

[22] J. W. Booth, J. C. Case, E. L. White, D. S. Shah, and R. Kramer-Bottiglio, "An addressable pneumatic regulator for distributed control of soft robots," in *2018 IEEE International Conference on Soft Robotics (RoboSoft)*. IEEE, 2018, pp. 25–30.

[23] E. Richer and Y. Hurmuzlu, "A high performance pneumatic force actuator system: Part i—nonlinear mathematical model," *J. dyn. sys., meas., control*, vol. 122, no. 3, pp. 416–425, 2000.

[24] S. V. Krichel and O. Sawodny, "Non-linear friction modelling and simulation of long pneumatic transmission lines," *Mathematical and Computer Modelling of Dynamical Systems*, vol. 20, no. 1, pp. 23–44, 2014.

[25] M. Turkseven and J. Ueda, "An asymptotically stable pressure observer based on load and displacement sensing for pneumatic actuators with long transmission lines," *IEEE/ASME transactions on mechatronics*, vol. 22, no. 2, pp. 681–692, 2016.

[26] D. Bruder, M. A. Graule, C. B. Teeple, and R. J. Wood, "Increasing the payload capacity of soft robot arms by localized stiffening," *Science Robotics*, vol. 8, no. 81, p. eadf9001, 2023. [Online]. Available: https://www.science.org/doi/abs/10.1126/scirobotics.adf9001

[27] B. Tondu, "Modelling of the mckibben artificial muscle: A review," *Journal of Intelligent Material Systems and Structures*, vol. 23, no. 3, pp. 225–253, 2012.

[28] D. Bruder and R. J. Wood, "The chain-link actuator: Exploiting the bending stiffness of mckibben artificial muscles to achieve larger contraction ratios," *IEEE Robotics and Automation Letters*, vol. 7, no. 1, pp. 542–548, 2021.

[29] R. Van Ham, B. Verrelst, F. Daerden, and D. Lefeber, "Pressure control with on-off valves of pleated pneumatic artificial muscles in a modular one-dimensional rotational joint," in *International conference on humanoid robots*, 2003, p. 35.

[30] F. Daerden, D. Lefeber, B. Verrelst, and R. Van Ham, "Pleated pneumatic artificial muscles: actuators for automation and robotics," in *2001 IEEE/ASME International Conference on Advanced Intelligent Mechatronics. Proceedings (Cat. No. 01TH8556)*, vol. 2. IEEE, 2001, pp. 738–743.

[31] S. Garrido-Jurado, R. Muñoz-Salinas, F. Madrid-Cuevas, and M. Marín-Jiménez, "Automatic generation and detection of highly reliable fiducial markers under occlusion," *Pattern Recognition*, vol. 47, no. 6, pp. 2280–2292, 2014. [Online]. Available: https://www.sciencedirect.com/science/article/pii/S0031320314000235

[32] R. M. Murray, Z. Li, and S. S. Sastry, *A mathematical introduction to robotic manipulation*. CRC press, 2017.

[33] E. Gallardo Hevia, C. M. McCann, M. Bell, N.-s. P. Hyun, C. Majidi, K. Bertoldi, and R. J. Wood, "High-gain microfluidic amplifiers: the bridge between microfluidic controllers and fluidic soft actuators," *Advanced Intelligent Systems*, vol. 4, no. 10, p. 2200122, 2022.

[34] T. Dai, N. Velimirović, P. Zalles, D. Bruder, K. Buffinton, R. B. Gillespie, and C. D. Remy, "Modeling and experimental validation of high-flow fluid-driven membrane valves for hyperactuated soft robots," *Advanced Intelligent Systems*, p. 2300864, 2024.